American Mineralogist, Volume 71, pages 1354–1365, 1986

Experimental study of cummingtonite and Ca-Na amphibole relations in the system Cum-Act-Pl-Qz-H_2O

TAKANOBU OBA,* IAN A. NICHOLLS
Department of Earth Sciences, Monash University, Clayton, Victoria 3168, Australia

ABSTRACT

Portions of the systems cummingtonite (Mg_{50})–actinolite (Mg_{50})–plagioclase (An_0, An_{20}, An_{40})–quartz–water have been studied within the melting range 700–850°C under a water pressure of 5 kbar and oxygen fugacities of the FMQ buffer. In the system Cum–Act–An_0–Qz–H_2O, cummingtonite coexists with a range of Ca-Na amphiboles, which themselves show continuous solid solution, but have a wide miscibility gap with respect to cummingtonite. At 700°C, mafic assemblages (coexisting with quartz, silica-rich liquid, and vapor) change as follows with increasing Act component: cummingtonite; cummingtonite + crossite + orthopyroxene; subcalcic amphibole + orthopyroxene; actinolite + Ca-clinopyroxene + orthopyroxene. Cummingtonite is present for bulk CaO contents to 3.4 wt%, and Ca in cummingtonite and Ca-Na amphibole correlates with bulk Ca content. At temperatures above 750–800°C, amphibole-bearing assemblages are replaced by Ca-clinopyroxene + orthopyroxene. In the corresponding systems with An_{20} and An_{40} components, cummingtonite is always accompanied by actinolite or actinolitic hornblende. With more calcic plagioclase components, Ca-amphibole stability increases, and the various stability fields of the An_0 system shift toward Cum-rich compositions.

Chemical compositions of amphiboles reflect their high temperatures of equilibration relative to metamorphic conditions, with either single-phase amphiboles lying within accepted miscibility gaps or coexisting amphiboles showing extensive mutual solid solution. Controls on miscibility of amphibole endmembers and the petrologic significance of amphibole pairs in metamorphic and volcanic rocks are discussed in the light of the experimental results.

INTRODUCTION

Coexisting Ca-rich and Ca-poor amphiboles occur widely in both metamorphic and igneous assemblages. Their compositional relationships in blueschists, greenschists, and mafic to intermediate amphibolites are known from microprobe studies of natural metamorphic assemblages (e.g., Klein, 1968; Stout, 1972; Spear, 1977, 1982). Spear (1977, 1981, 1982) analyzed the theoretical phase relations of amphibolite-facies assemblages and experimentally studied compositional variation in hornblendes of these assemblages. Cameron (1975) investigated in detail the experimental subsolidus stability and compositional relations of coexisting Ca-poor and Ca-rich amphiboles on the join $(Mg,Fe)_7Si_8O_{22}(OH)_2$-$Ca_2(Mg,Fe)_5Si_8O_{22}(OH)_2$ at P_{H_2O} = 2 kbar. He reported that cummingtonite and actinolite are separated by a solvus and that the maximum solubility of cummingtonite component in actinolite is reached at 600°C ($Act_{85\pm4}$).

Ewart (1971) and Ewart et al. (1971, 1975) described the phenocryst assemblages cummingtonite + orthopyroxene and cummingtonite + hornblende + orthopyroxene from rhyolites and pumices of the Taupo volcanic zone, New Zealand, and investigated the conditions under which these were equilibrated. Similar assemblages were studied by d'Arco et al. (1981) and Pedersen and Hald (1982). These assemblages are not represented in the phase diagram reported by Cameron (1975), and no other systematic experimental studies have examined the stability and compositional relationships of coexisting cummingtonite and Ca-Na amphibole in the presence of liquid. Therefore, phase stability and compositional relations of cummingtonite and Ca-amphiboles have been studied in the presence of liquid within the system Cum-Act-Pl-Qz-H_2O at P_{H_2O} = 5 kbar, 700–850°C.

EXPERIMENTAL METHODS

Synthetic amphibole components with $Mg/(Mg + Fe_{tot}) = 0.5$ were combined with plagioclase components An_0, An_{20}, and An_{40} and silica, in bulk compositions chosen to yield model rhyolitic liquids coexisting with amphiboles and pyroxenes over wide temperature ranges (Table 1). Most experiments were carried out along three joins—$(Cum\text{-}Act)_{40}(An_0)_{40}Qz_{20}$, $(Cum\text{-}Act)_{35}(An_{20})_{40}Qz_{25}$, and $(Cum\text{-}Act)_{30}(An_{40})_{40}Qz_{30}$. Starting materials were first prepared by passing H gas over fine-grained sintered oxide mixtures at 1100°C for ~5 h. These were combined in the required proportions, then crystallized with excess water

* Present address: Institute of Geosciences, University of Joetsu Education, Joetsu, Nigata 943, Japan.

0003–004X/86/1112–1354$02.00

in a 0.5-in.-diameter piston-cylinder high-pressure apparatus. Furnace assemblies consisted of a talc sleeve enclosing a graphite heater (5.6-mm internal diameter) sandwiched between 1-mm-thick Pyrex glass sleeves. Sample and buffer capsule assemblies were located within the furnace hot-zone between a lower pressed NaCl rod and upper Pyrex thermocouple guide. Space around the sides and lower ends of capsule assemblies was packed with NaCl powder. Use of this furnace configuration with a −10% piston-in "friction" correction allowed the quartz-coesite transition to be accurately located within a 1-kbar bracket. A Pt/Pt–10% Rh thermocouple was isolated from the sample capsule assembly by a mullite disc and used with a Leeds and Northrup Electromax II unit to control temperature to within ±10°C.

A double-capsule configuration with FMQ buffer + H_2O in the outer capsule was used to control f_{H_2}. Inner capsules were 2.0-mm-diameter $Ag_{50}Pd_{50}$ alloy; outer capsules were 3.5-mm pure Ag. Two inner capsules were used for reversal experiments (see below) and for pairs of charges defining the stability limits of a particular phase at the same temperature. With two capsules, restrictions on the amount of buffer that could be loaded allowed only short run times to be used.

At the completion of each run, the capsule assembly was weighed to check that water had not been lost from the buffer, then the buffer material was examined optically to confirm the persistence of the full FMQ assemblage. X-ray diffractometer traces for buffer material in selected runs showed that the proportion of fayalite decreased with time. Charges from sample capsules were studied in detail by optical microscope, X-ray diffractometer, and electron microprobe. Optical distinction between Ca-amphibole, Ca-Na amphibole, and cummingtonite was difficult, in spite of the faint green color of the Ca-bearing varieties. The position of the 310 Cu$K\alpha$ X-ray diffraction peak for the Ca-amphibole and Ca-Na amphiboles at about 28.5° 2θ, compared with about 29.0° for cummingtonite, is a more reliable discriminant. Intergrowths between amphiboles (see below) were recognized optically and studied in detail using back-scattered electron imaging by microprobe.

To assess approach to equilibrium in synthesis experiments, several series of runs of increasing duration were carried out on two bulk compositions—$(Cum_{1.0}Act_{0.0})_{40}(An_{40})_{40}Qz_{20}$ and $(Cum_{0.5}Act_{0.5})_{40}(An_{40})_{40}Qz_{20}$—at 700°C, and the compositions of resulting amphiboles were monitored by microprobe analysis. Assemblages including cummingtonite for the first of these compositions (run durations 48–240 h) and Ca-Na amphibole and cummingtonite for the second (24–144 h) show little change in grain size and texture, and no systematic change in amphibole compositions (Fig. 1). In the single experiment run for 240 h, the FMQ buffer was exhausted, leading to the crystallization of

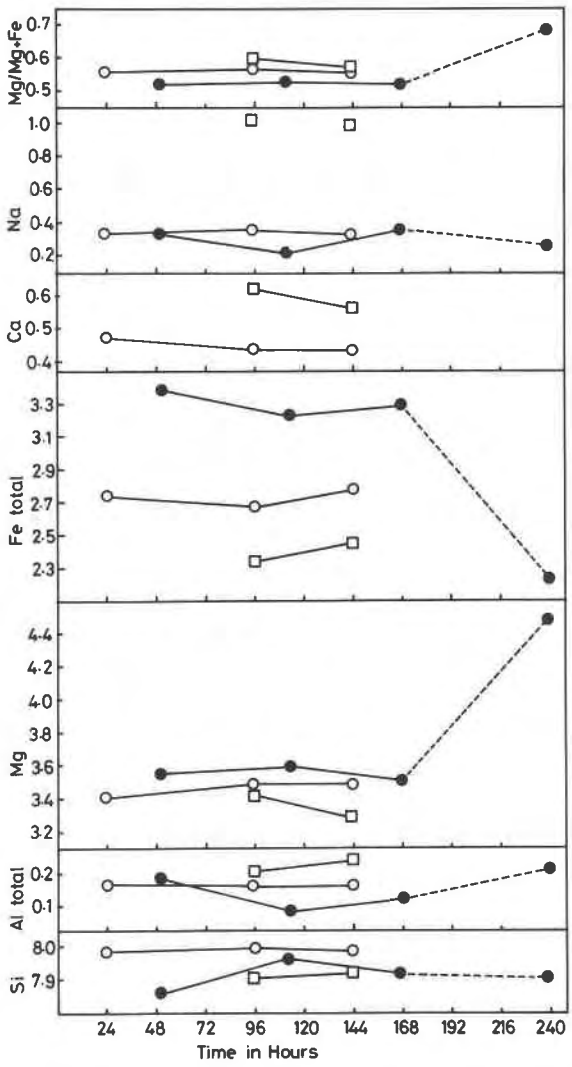

Fig. 1. Amphibole compositions as a function of run duration in hours, under conditions of T = 700°C, P_{H_2O} = 5 kbar, f_{H_2} = FMQ. Solid circles: cummingtonite—charge composition $Cum_{40}(An_0)_{40}Qz_{20}$. Open circles and squares: cummingtonite and Ca-Na amphibole, respectively—charge composition $(Cum_{0.5}Act_{0.5})_{40}(An_0)_{40}Qz_{20}$. Dashed line: changes due to exhaustion of buffer.

Table 1. Endmember compositions used in studies of amphibole stability in the system anhydrous Cum–anhydrous Act–Pl–Qz–H_2O

	1	2	3	4	5	6
	Proportions (wt%) and compositions (mol%) of components					
Cum (Mg_{50})	40	—	35	—	30	—
Act (Mg_{50})	—	40	—	35	—	30
Pl	40 (An_0)	40 (An_0)	40 (An_{20})	40 (An_{20})	40 (An_{40})	40 (An_{40})
Qz	20	20	25	25	30	30
	Bulk compositions (wt%)					
SiO_2	69.5	69.5	69.7	69.7	69.8	69.8
Al_2O_3	7.8	7.8	9.2	9.2	10.6	10.6
FeO	11.5	8.2	10.1	7.2	8.6	6.2
MgO	6.5	4.6	5.7	4.0	4.8	3.5
CaO	0	5.1	1.6	6.1	3.3	7.2
Na_2O	4.7	4.7	3.8	3.8	2.8	2.8

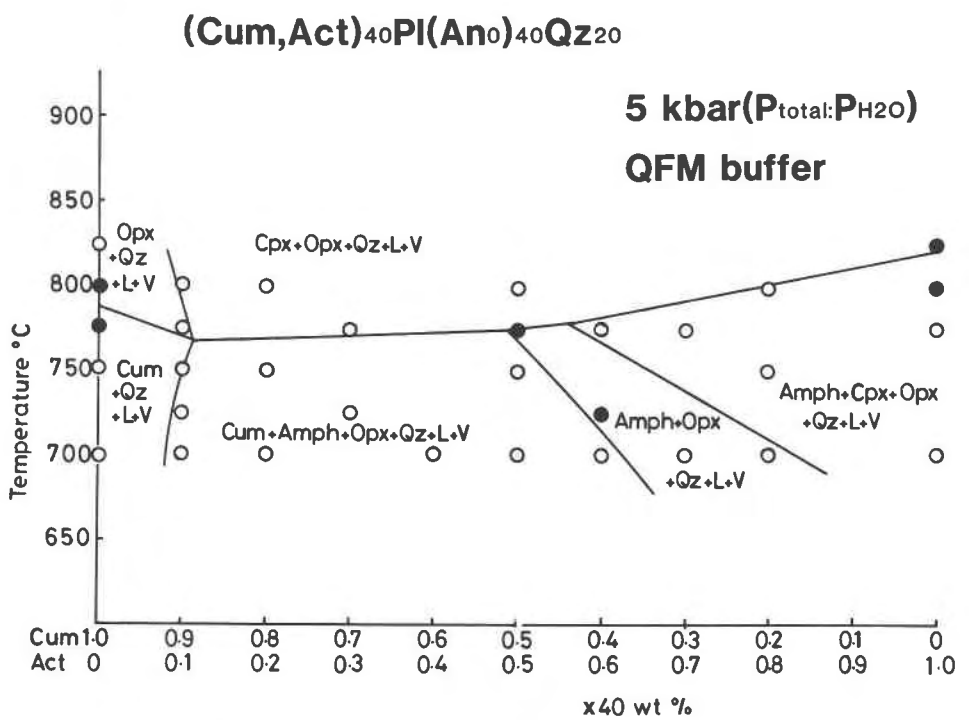

Fig. 2. *T-X* diagram for the join $Cum_{40}(An_0)_{40}Qz_{20}$-$Act_{40}(An_0)_{40}Qz_{20}$ (weight proportions) at P_{H_2O} = 5 kbar, f_{H_2} = FMQ. Solid circles indicate reversal experiments.

magnetite, and the formation of anomalously magnesian cummingtonite (dashed line, Fig. 1).

Reversal experiments were carried out on selected phase boundaries, e.g., the stability limit of cummingtonite for the bulk composition $(Cum_{1.0}Act_{0.0})_{40}(An_0)_{40}Qz_{20}$ (Fig. 2). The assemblage Opx + Qz + L + V that previously formed at 800°C was run at 775°C. Cum appeared, and the amount of Opx present decreased. When the 775°C assemblage Cum + Qz + L + V was run at 800°C, Cum disappeared and Opx crystallized. These and similar results indicate a close approach to equilibrium for the conditions and run durations used.

The chemical compositions of the experimental amphiboles, and coexisting phases (Table 2), were determined using a Bausch and Lomb SEMQ2 electron microprobe fitted with a Microtrace energy-dispersive X-ray detector and Inotech Ultima II multichannel analyzer. Instrument operating conditions were 15-kV accelerating voltage, 5-nA beam current, 50-s live counting time. The low beam current, finely focused (~1 μm) beam, and short counting time allowed resolution of amphibole intergrowths in back-scattered electron images at magnifications of 2000–5000× (see below). Amphibole compositions given in Table 3 represent the average of several grains or areas within intergrowths.

Nature of experimental products

Total crystal proportions in experimental charges range up to 90% in some 700°C assemblages. Cummingtonite and Ca-Na amphiboles form fibrous crystals of ~15-μm maximum length and ~5-μm diameter. When the two amphiboles coexist, they commonly occur as parallel intergrowths. By contrast, Ca-amphibole typically forms independent bladed crystals up to 25 μm in length and 10 μm in maximum diameter. Calcic clinopyroxene and orthopyroxene form shorter, broader prismatic crystals. Quartz occurs as granular crystals to 10 μm. Areas of glass in most charges are uniform and colorless, with abundant vapor bubbles. Minor quench crystallization of fibrous cummingtonite was observed in only one charge.

Experimental results

Cum-Act-An_0-Qz-H_2O

Experimental results for the An_0 system at 5-kbar P_{H_2O} are listed in Table 2, and Figure 2 shows the phase diagram based on these. Cummingtonite is the sole amphibole stable for Cum-rich compositions, and it coexists with Ca- or Na-amphibole to bulk compositions with 50–60 mol% Act. At 700°C it is lost from the assemblages when CaO content in the bulk composition is higher than about 3.3 wt%. Phase assemblages at 700°C change as follows with increasing bulk Act content: Cum + Qz + L + V, Na-Amph + Cum + Opx + Qz + L + V, subcalcic Amph + Opx + Qz + L + V, and Act + Cpx + Opx + Qz + L + V. The assemblages Opx + Qz + L + V and Cpx + Opx + Qz + L + V are high-temperature decomposition products of these amphibole-bearing assemblages. In Figure 3, quartz-saturated phase relations of coexisting amphiboles and pyroxenes are represented in projection onto the plane $Ca_7Si_8O_{23}$-$Mg_7Si_8O_{23}$-$Fe_7Si_8O_{23}$ (Cameron, 1975). Phase relations along the join $Mg_{3.5}Fe_{3.5}Si_8O_{22}(OH)_2$-$Ca_2Mg_{2.5}Fe_{2.5}Si_8O_{22}(OH)_2$ of Figure 3 are based on those of Figure 2. Since no experimental stability field of Cum + Opx + Qz + L + V has been observed (Table 2, Fig. 2), the Cum apex of the compatibility triangle Ca-Na Amph–Cum–Opx has been drawn to lie exactly on the compositional join. The phase assem-

Table 2. Experimental results for Cum-Act-Pl-Qz systems at 5-kbar P_{H_2O}

Run no.	Composition (wt%) Cum	Act	T (°C)	Time (h)	Assemblage (including Gl, V)
			$(Cum,Act)_{40}(An_0)_{40}Qz_{20}$		
71	100	0	700	116	Cum, (Opx), Qz
37			700	168	Cum, Qz
15			700	240	Cum, Opx, Mt
1			750	144	Cum, Qz
23			775	96	Cum, Qz
18			800	96	Opx, Qz
2	90	10	700	116	Cum, Qz
7			725	140	Cum, Amph, Opx, Qz
5			750	72	Cum, Opx, Qz
20			775	53	Opx, Qz
21			800	24	Opx, tr. Cpx, Qz
19	80	20	700	148	Cum, Amph, Opx, Qz
10			750	150	Cum, tr. Amph, (Cpx), Opx, Qz
22			800	32	Cpx, Opx, Qz
8	70	30	725	90	Cum, Amph, Opx, Qz
9			775	96	Cpx, Opx, Qz
26	60	40	700	144	Cum, Amph, Opx, Qz
85	50	50	700	24	Cum, tr. Amph, Opx, Pl
86			700	96	Cum, Amph, Opx, Qz
32			700	144	Cum, Amph, Opx, Qz
14			750	72	Cum, Amph, Opx, Qz
12			775	48	Amph, (Cpx), Opx, Qz
60			775	78	Amph, Opx, Qz
11			800	50	Cpx, Opx, Qz
31	40	60	700	144	Cum, Amph, Opx, Qz
35			725	120	Amph, Opx, Qz
61			775	24	Amph, Opx, (Cpx), Qz
41			775	72	Amph, Opx, Qz
68	30	70	700	120	Amph, Opx, Qz
62			775	48	Amph, Cpx, Opx, Qz
30	20	80	700	144	Amph, Opx, Qz
36			750	120	Amph, Cpx, Opx
34			800	24	Amph, Cpx, Opx
25	0	100	700	168	Amph, Cpx, Qz
29			775	55	Amph, Cpx, Opx, Qz
16			800	96	tr. Amph, Cpx, Opx, Qz
17			825	36	Cpx, Opx, Qz
			$(Cum,Act)_{35}(An_{20})_{40}Qz_{25}$		
7	100	0	700	168	Cum, Amph, Opx, Qz
23			825	36	Cpx, Opx, Qz, Mt
4	90	10	700	168	Cum, Amph, Opx, Qz
3			800	72	Cum, Amph, Opx, Qz
31			850	36	Cpx, Opx, Qz
46	80	20	750	60	Cum, Amph, Opx, Qz
26			800	30	Amph, Cpx, Opx, Qz
32			825	36	tr. Amph, Cpx, Opx, Qz, Mt
5	70	30	700	96	Cum, Amph, Opx, Qz
30			725	120	Amph, Opx, Qz
10			750	57	Amph, Cpx, Opx, Qz
9			800	20	Amph, Cpx
27	60	40	700	144	Amph, Cpx, Opx, Qz
25			850	20	Cpx, Qz
1	40	60	700	144	Amph, Cpx, Opx, Qz
6			750	120	Amph, Cpx, Opx, Qz
			$(Cum,Act)_{30}(An_{40})_{40}Qz_{30}$		
1	100	0	700	144	Cum, Amph, (Cpx), Opx, Qz
3			750	72	Amph, Opx, Qz
5			800	78	Cpx, Opx, Qz
2	90	10	700	144	Amph, Cpx, Opx, Qz
6			775	98	Cpx, Opx, Qz
4	80	20	775	48	Amph, Cpx, Opx, Qz
7			800	24	Cpx, Opx, Qz
			Reversal runs		
			$(Cum,Act)_{40}(An_0)_{40}Qz_{20}$		
33	100	0	800	24	Cum, Qz → tr. Cum, Opx, Qz
24			775	55	Opx, Qz → Cum, (Opx), Qz
65	50	50	775	55	Cpx, Opx, Qz → Amph, Opx, Qz
66	40	60	725	120	Cum, Amph, Opx, Qz → Amph, Opx, Qz
42	0	100	800	24	Cpx, Opx, Qz → Amph, Cpx, Opx, Qz
43			825	24	Amph, Cpx, Opx, Qz → Cpx, Opx, Qz
			$(Cum,Act)_{35}(An_{20})_{40}Qz_{25}$		
28	100	0	825	36	Cum, Amph, Opx, Qz → Cpx, Opx, Qz, Mt
29	80	20	825	36	Cpx, Opx, Qz → Amph, Cpx, Opx, Qz, Mt
45	70	30	700	144	Amph, Opx, Qz → Cum, Amph, Opx, Qz
			$(Cum,Act)_{30}(An_{40})_{40}Qz_{30}$		
19	100	0	700	120	Amph, Opx, Qz → Amph, Cum, Opx, Qz
9	80	20	800	36	Amph, Cpx, Opx, Qz → Cpx, Opx, Qz

Abbreviations: Cum, cummingtonite. Amph, Ca-Na clinoamphibole. Opx, orthopyroxene. Cpx, Ca clinopyroxene. Qz, quartz. Pl, plagioclase. Mt, magnetite. Gl, glass. V, quenched vapor. tr., trace.

blages obtained differ from those found experimentally by Cameron (1975) on the join cummingtonite (Mg_{50})-actinolite (Mg_{50}), at 2 kbar and similar temperatures. In the present experiments the tie line Ca-Amph–Opx is stable, whereas in those of Cameron, this is replaced by the stable tie line Ca-Cpx–Cum. In the Act-rich portion of Figure 2, there is no stability field of cummingtonite at temperatures higher than those of Ca-Na amphibole. By contrast, Cameron (1975) reported that actinolite decomposed at temperatures above 700°C by the reaction Act → Cum + Cpx + Qz + V.

The average chemical compositions of experimental amphiboles in the system Cum-Act-An_0-H_2O are listed in Table 3. The corresponding structural formulae assume Fe^{2+} = total Fe, but values of the ratio $Fe^{3+}/(Fe^{3+} + Fe^{2+})$ calculated from average Fe^{3+} contents estimated by the RECAMP recalculation procedures of Spear and Kimball (1984) are also given, along with resulting $Mg/(Mg + Fe^{2+})$

Table 3. Chemical compositions of amphiboles synthesized at 5-kbar P_{H_2O}

	1 (11) Cum	2 (11) Cum	3 (6) Cum	4 (21) Cum	5 (12) Cum	6 (5) Cros	7 (13) Cum	8 (4) Win	9 (10) Win	10 (20) Cum	11 (5) Win	12 (16) Cum	13 (5) Win	14 (14) Cum	15 (8) Win
	Cum-Act-An_0-Qz system														
	1.0* 0.0† 700°C	1.0* 0.0† 750°C	1.0* 0.0† 775°C	0.9* 0.1† 700°C	0.8* 0.2† 700°C	0.8* 0.2† 700°C	0.8* 0.2† 750°C	0.8* 0.2† 750°C	0.7* 0.3† 725°C	0.6* 0.4† 700°C	0.6* 0.4† 700°C	0.5* 0.5† 700°C	0.5* 0.5† 700°C	0.5* 0.5† 750°C	0.5* 0.5† 750°C
SiO_2	52.85	54.45	54.88	53.87	54.19	51.43	53.44	55.09	54.22	54.13	54.92	54.12	55.22	53.83	54.12
Al_2O_3	0.70	0.71	0.80	0.87	0.70	9.30	0.78	2.69	3.69	0.92	2.36	0.95	1.46	1.03	0.75
FeO	26.27	24.31	23.35	25.76	23.43	17.78	24.42	21.05	21.54	23.79	22.28	22.43	20.41	22.11	21.33
MgO	15.69	17.41	17.86	16.10	16.29	13.37	16.71	15.30	15.16	16.04	14.64	15.64	15.34	16.39	16.54
CaO	0	0	0	0.18	0.65	0.45	0.44	0.46	1.20	1.61	1.34	2.66	3.62	2.13	1.88
Na_2O	1.22	0.96	1.03	0.83	1.38	6.71	0.69	2.81	4.02	0.77	3.64	1.14	3.55	1.02	2.35
Total	96.73	97.84	97.92	97.61	96.64	99.04	96.48	97.40	99.83	97.26	99.18	96.93	99.60	96.51	96.97
	Structural formulae calculated on the basis of 23 oxygens														
Si T	7.920	7.958	7.972	7.947	8.014	7.343	7.944	7.991	7.757	7.972	7.923	7.982	7.924	7.953	7.961
Al	0.080	0.042	0.028	0.053	—	0.657	0.056	0.009	0.243	0.028	0.077	0.018	0.076	0.047	0.039
Al M1, M2, M3	0.044	0.080	0.109	0.098	0.122	0.908	0.081	0.451	0.379	0.132	0.324	0.147	0.171	0.132	0.175
Mg	3.505	3.793	3.868	3.541	3.591	2.846	3.703	3.308	3.233	3.522	3.148	3.439	3.282	3.610	3.627
Fe	1.451	1.127	1.023	1.361	1.287	1.246	1.216	1.241	1.388	1.346	1.528	1.414	1.547	1.258	1.198
Fe M4	1.841	1.844	1.814	1.817	1.611	0.877	1.820	1.312	1.189	1.584	1.160	1.353	0.902	1.474	1.426
Ca	0	0	0	0.028	0.103	0.069	0.070	0.071	0.183	0.254	0.207	0.420	0.557	0.337	0.296
Na	0.159	0.156	0.186	0.155	0.286	1.054	0.110	0.617	0.628	0.162	0.633	0.227	0.541	0.189	0.278
Na A	0.195	0.116	0.104	0.082	0.110	0.804	0.089	0.173	0.487	0.058	0.385	0.099	0.447	0.103	0.392
Ca	—	—	—	—	—	—	—	—	—	—	—	—	—	—	—
Total	15.195	15.116	15.104	15.082	15.124	15.804	15.089	15.173	15.487	15.058	15.385	15.099	15.447	15.103	15.392
Mg	51.6	56.1	57.7	52.7	55.3	57.3	54.9	56.4	55.6	54.6	53.9	55.4	57.3	56.9	58.0
Fe	48.4	43.9	42.3	47.3	44.7	42.7	45.1	43.6	44.4	45.4	46.1	44.6	42.7	43.1	42.0
Ca	0	0	0	0.4	1.6	1.4	1.0	1.2	3.1	3.8	3.4	6.3	8.9	5.0	5.6
Mg	51.6	56.1	57.7	52.5	54.5	56.5	54.4	55.8	53.9	52.5	52.1	51.9	52.2	54.1	54.8
Fe	48.4	43.9	42.3	47.1	43.9	42.1	44.6	43.0	43.0	43.7	44.5	41.8	38.9	40.9	39.6
$Fe^{3+}/(Fe^{3+} + Fe^{2+})$	0.038	0.060	0.056	0.044	0.079	0.500	0.044	0.105	0.291	0.030	0.220	0.054	0.201	0.058	0.100
$Mg/(Mg + Fe^{2+})$	52.5	57.6	59.1	53.8	57.4	72.8	56.1	59.1	63.9	55.3	60.0	56.8	62.6	58.4	60.6

values. According to the classification of Leake (1978), the Ca-amphibole is an actinolite, whereas the subcalcic amphibole is similar to winchite. The Na-rich amphibole may be a solid solution between Na cummingtonite (or Na anthophyllite) and crossite. The Mg-Fe amphibole is invariably cummingtonite.

As the most important distinction between the major amphibole groups is in the occupancy of the M4 site, the experimental amphiboles are plotted in terms of relative proportions of Na, (Mg + Fe^{2+}), and Ca in the M4 site in Figure 4, using Fe^{2+} = total Fe (Fig. 4A) and estimated Fe^{2+} (and Fe^{3+}) contents (Fig. 4B). In natural amphibole-bearing assemblages from metamorphic rocks there is a notable lack of solid solution between the Mg-Fe and Ca-Na amphiboles (Robinson et al., 1982). The maximum Ca contents of the synthetic cummingtonites are appreciably higher than those in natural metamorphic equivalents, presumably reflecting their relatively high temperatures of formation (see Discussion).

Figure 5 shows Ca, Na, and total Al contents in Ca-Na amphibole and cummingtonite plotted against the respective bulk compositions. The experimental results suggest that there is a continuous solid-solution series between crossite and actinolite. The Ca content of Ca-Na amphibole increases rapidly in parallel with that of the bulk composition, while Na and Al both decrease. There is a systematic chemical variation between crossite and actinolite. The Ca content of cummingtonite increases with increasing bulk-system Ca content, with Na and Al low and approximately constant. These systematic compositional variations shown by Ca-Na amphibole and cummingtonite suggest that microprobe analysis using back-scattered electron images has satisfactorily resolved the two phases present in lamellar intergrowths and that the narrow miscibility gaps of Figure 4 do not result from mixed analyses.

Cum-Act-An_{20}-Qz-H_2O

The phase diagram for the An_{20} system (Fig. 6) shows that the stability relations are similar to those of the central part of the corresponding diagram for the An_0 system (Fig. 3). Cummingtonite again disappears for bulk CaO contents greater than 3.2 wt% at 700°C. Magnetite appears at 825°C in the cummingtonite-rich portion of this system.

The chemical compositions and structural formulae of amphiboles in the An_{20} system are given in Table 3. According to the Leake classification, the Ca amphibole is an actinolitic hornblende (AcHbl), and the Mg-Fe am-

Table 3—*Continued*

16 (11) Cum	17 (6) Act	18 (7) Act	19 (12) Act	20 (4) Cum	21 (21) Hbl	22 (4) Cum	23 (6) Hbl	24 (9) Cum	25 (8) Hbl	26 (9) Hbl	27 (5) Cum	28 (6) Hbl	29 (16) Hbl	30 (6) Hbl	31 (11) Hbl
Cum-Act-An_0-Qz (*continued*)				Cum-Act-An_{20}-Qz system							Cum-Act-An_{40}-Qz system				
0.4* 0.6† 700°C	0.4* 0.6† 700°C	0.2* 0.8† 700°C	0* 1.0† 700°C	0.9* 0.1† 700°C	0.9* 0.1† 700°C	0.9* 0.1† 800°C	0.9* 0.1† 800°C	0.7* 0.3† 800°C	0.7* 0.3† 700°C	0.4* 0.6† 700°C	1.0* 0† 700°C	1.0* 0† 700°C	1.0* 0† 750°C	0.9* 0.1† 700°C	0.8* 0.2† 775°C
53.72	54.24	54.95	56.29	51.48	51.18	52.05	50.99	50.29	48.99	48.90	52.74	49.43	48.33	50.63	49.66
0.86	1.64	1.18	0.57	3.74	4.99	4.18	6.53	4.34	6.02	5.56	2.80	6.74	7.36	8.08	6.21
23.29	21.47	18.33	7.83	24.16	19.53	22.84	17.17	24.64	20.12	19.16	25.17	17.67	19.45	18.41	18.06
15.63	14.11	13.92	19.84	14.65	13.56	15.22	14.31	13.93	12.71	11.85	13.98	12.15	11.39	10.78	13.24
3.14	4.23	7.48	11.08	3.05	9.29	3.42	8.64	2.61	8.56	10.51	1.49	10.34	9.25	9.63	8.52
1.16	3.04	2.32	0.79	0.29	0.62	0.28	0.58	0.55	0.80	1.04	0.70	0.89	1.23	1.13	0.80
97.80	98.73	98.18	96.40	97.61	99.17	97.99	98.22	96.36	97.20	97.02	96.88	97.22	97.01	98.66	96.49
Structural formulae calculated on the basis of 23 oxygens															
7.909	7.903	7.982	7.975	7.631	7.437	7.615	7.374	7.562	7.300	7.323	7.846	7.306	7.217	7.350	7.367
0.091	0.097	0.018	0.025	0.369	0.563	0.385	0.626	0.438	0.700	0.677	0.154	0.694	0.783	0.650	0.633
0.058	0.185	0.184	0.070	0.284	0.292	0.336	0.487	0.331	0.357	0.304	0.337	0.480	0.512	0.732	0.453
3.430	3.065	3.014	4.190	3.237	2.937	3.319	3.085	3.123	2.824	2.645	3.101	2.677	2.536	2.333	2.928
1.512	1.750	1.802	0.740	1.479	1.771	1.345	1.428	1.546	1.819	2.051	1.562	1.843	1.952	1.935	1.619
1.355	0.866	0.425	0.189	1.516	0.602	1.449	0.649	1.553	0.688	0.349	1.570	0.341	0.477	0.300	0.622
0.495	0.666	1.164	1.682	0.484	1.398	0.536	1.339	0.420	1.312	1.651	0.238	1.637	1.480	1.498	1.354
0.150	0.468	0.411	0.129	—	—	0.015	0.012	0.027	—	—	0.192	0.022	0.043	0.202	0.024
0.181	0.391	0.242	0.088	—	0.048	—	—	—	0.055	0.035	—	—	—	—	—
—	—	—	—	0.083	0.175	0.064	0.151	0.133	0.231	0.302	0.010	0.233	0.313	0.116	0.206
15.181	15.391	15.242	15.088	15.083	15.223	15.064	15.151	15.133	15.286	15.337	15.010	15.233	15.313	15.116	15.206
54.5	54.0	57.6	81.9	51.9	55.3	54.3	59.8	50.2	53.0	52.4	50.2	55.1	51.1	51.1	56.6
45.5	46.0	42.4	18.1	48.1	44.7	45.7	40.2	49.8	47.0	47.6	49.8	44.9	48.9	48.9	43.4
7.3	10.5	18.2	24.7	7.2	21.4	8.1	20.6	6.3	20.4	25.0	3.7	25.2	22.9	24.7	20.8
50.5	48.3	47.1	61.6	48.2	43.5	49.9	47.5	47.0	42.2	39.3	47.9	41.2	39.2	38.5	44.9
42.2	41.2	44.7	13.7	44.6	35.1	32.0	31.9	46.7	37.4	35.7	48.4	33.6	37.9	36.8	34.3
0.058	0.204	0.167	0.142	0.043	0.175	0.035	0.111	0.066	0.209	0.239	0.004	0.164	0.198	0.080	0.140
55.9	59.5	61.9	84.0	53.0	60.0	55.8	62.6	51.9	58.7	59.1	49.9	59.5	56.5	53.2	60.3

Note: Each column is headed by its number followed by the number of analyses in parentheses. Abbreviations of synthesized amphiboles: Cum = cummingtonite; Cros = crossite; Win = winchite; Act = actinolite; Hbl = hornblende. Fe^{3+} and Fe^{2+} calculated by RECAMP (Spear and Kimball, 1984).
* Cum component in starting composition. † Act component in starting composition.

phibole is again a cummingtonite. These limited analytical data for the relatively narrow range of bulk compositions studied experimentally suggest that actinolitic hornblende shows less-pronounced dependence on system composition (Fig. 7) than does Ca-Na amphibole in the An_0 system (Fig. 5). As expected, the Ca content of the amphibole increases with that of the bulk composition. However, both Al and Na show parallel slight increases that are opposite to their behavior in the An_0 system. The available data for cummingtonite in only two bulk compositions ($Cum_{0.9}$ and $Cum_{0.7}$) are not sufficient to define reliable trends, but Ca and Al contents are higher, and Na contents are lower, than for cummingtonite in the An_0 system. These differences in cummingtonite appear to directly reflect the influence of bulk An content.

The reasons for the contrasted variation of Ca-Na amphibole and Ca-amphibole compositions in the An_0 and An_{20} systems are not clear. The rapid decrease in Na and Al contents with increasing Ca in Ca-Na amphiboles of the An_0 system, coupled with the almost constant Na and Al contents of coexisting cummingtonite, could be compatible with the appearance of another Na- and Al-rich phase, presumably Ab-rich plagioclase. However, this has been identified in only one assemblage (Table 2). Variation in the proportion and composition of liquid must be taken into account in interpreting amphibole trends. This will be attempted in a companion paper.

The amphiboles from the An_{20} system are plotted in terms of the relative proportions of Na, Ca, and (Mg + Fe^{2+}) in the M4 site in Figure 8, again using both Fe^{2+} = total Fe (Fig. 8A) and estimated Fe^{3+} contents (Fig. 8B). Since Fe^{3+} contents are low in both Cum and AcHbl, they have little influence on plotted positions. The miscibility gap between Ca-amphibole and Mg-Fe amphibole is only slightly narrower than that observed in natural metamorphic assemblages, largely owing to the relative richness of cummingtonites in Ca.

Cum-Act-An_{40}-Qz-H_2O

The diagram for the Cum-rich portion of the An_{40} system (Fig. 9) shows that phase relations are again similar to those in Figures 2 and 6, but stability fields are again

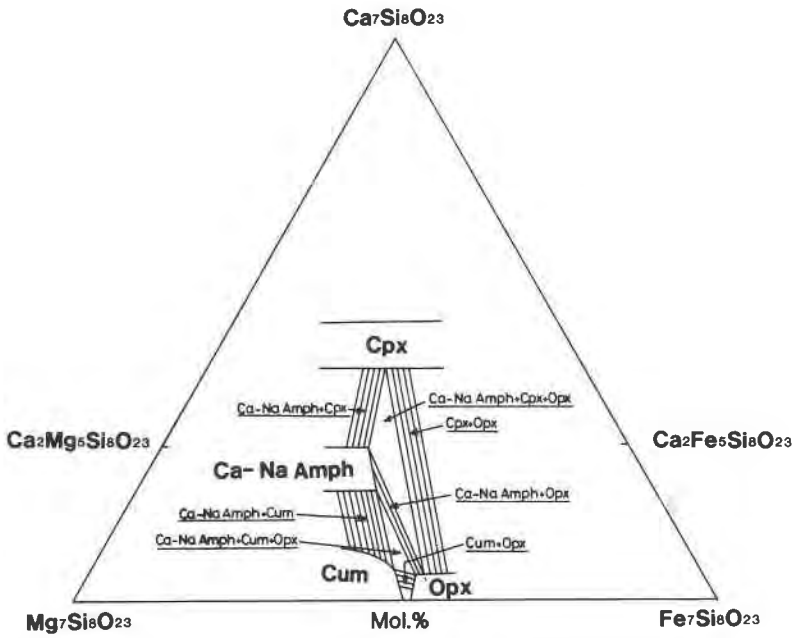

Fig. 3. Isothermal, isobaric compatibility diagram showing phase relations encountered in the present experimental study. All assemblages coexist with quartz, silica-rich liquid, and water-rich vapor.

shifted further toward the Cum endmember. Cummingtonite is lost from assemblages at 700°C when the CaO content of the bulk composition is greater than 3.4%. The available analytical data for Ca-amphibole (hornblende) in two An_{40} bulk compositions ($Cum_{1\,0}$ and $Cum_{0\,9}$) show that whereas Ca and Na contents (Fig. 10) are similar to those of equivalent amphiboles in the An_{20} system (Fig. 7), Al contents are appreciably higher. The coexisting

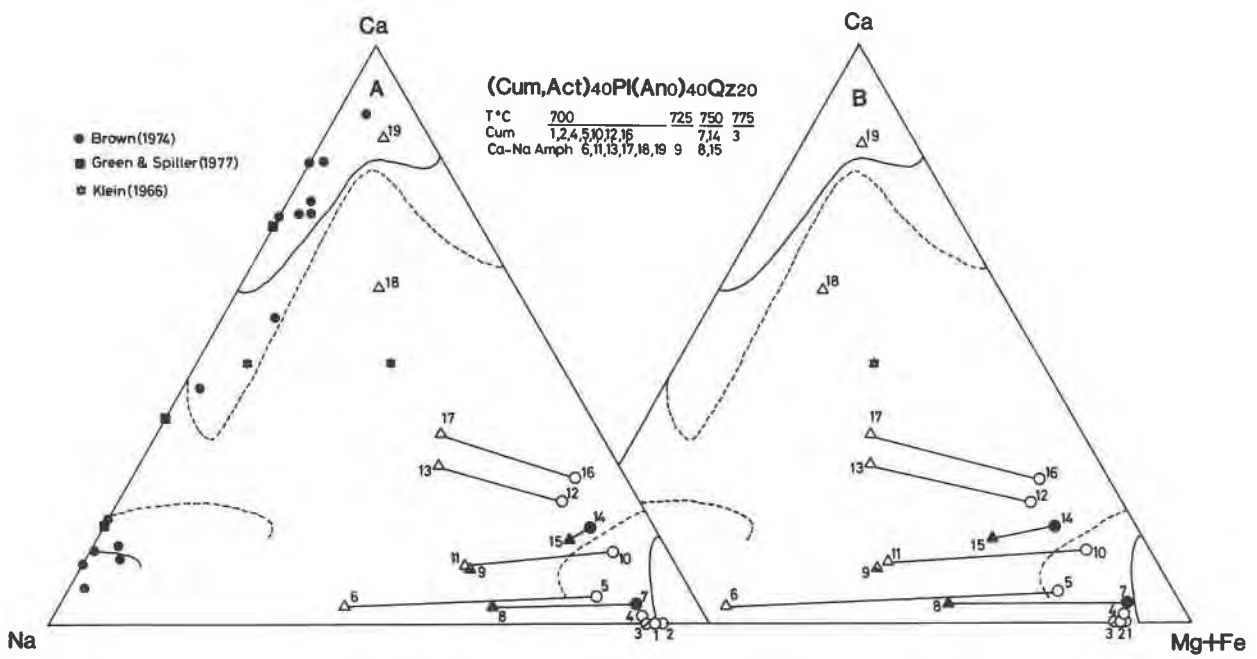

Fig. 4. Relative proportions of Ca, Na, and (Mg + Fe^{2+}) in the M4 site for coexisting amphiboles in the system $Cum_{40}(An_0)_{40}Qz_{20}$-$Act_{40}(An_0)_{40}Qz_{20}$. Field boundaries are those for representative microprobe analyses (solid lines) and wet-chemical analyses (dashed lines) for coexisting amphiboles of a variety of occurrences (Robinson et al., 1982, Fig. 20). (A) Fe^{2+} equals total Fe. (B) Fe^{2+} and Fe^{3+} (average) calculated by the computer program RECAMP of Spear and Kimball (1984). References given for selected comparative compositions.

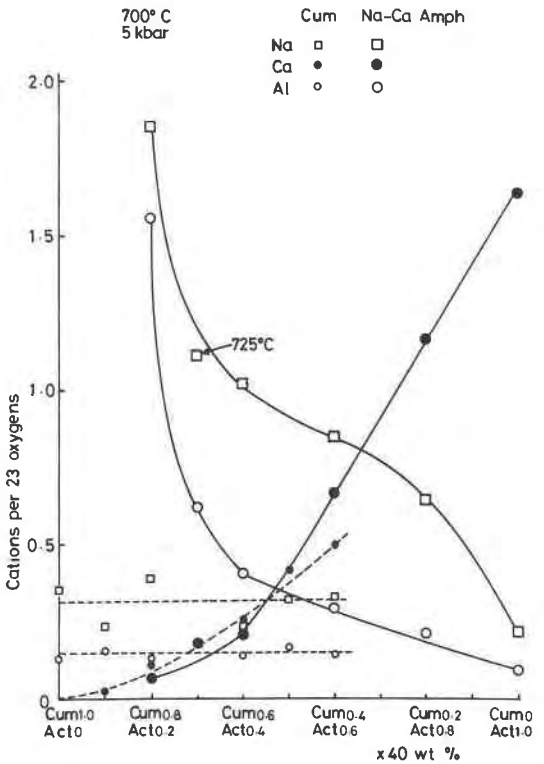

Fig. 5. Variation in proportions of Na, Ca, and Al on the basis of 23 oxygens as a function of system bulk composition for cummingtonites and Ca-Na amphiboles in the system Cum-Act-(An_0)-Qz at 5-kbar P_{H_2O}, 700°C [725°C for the bulk composition $(Cum_{0.7}Act_{0.3})_{40}(An_0)_{40}Qz_{20}$]. Symbols for the two amphiboles and each cation shown in the legend.

cummingtonite in the $Cum_{1.0}$ composition has lower Ca and Al and slightly higher Na than the equivalents in the An_{20} system. Again, detailed interpretation of these compositional trends requires consideration of the effect of coexisting liquid on mass balance.

The amphibole data for the An_{40} system plot close to those for the An_{20} system in Figure 8, and they define a similar miscibility gap between Ca-amphiboles and Mg-Fe amphiboles.

Discussion

Actinolite-crossite relationships

The existence of compositional gaps between coexisting sodic (glaucophane-crossite) and calcic-sodic amphiboles (actinolite, hornblende), at least at temperatures <550°C, is well established (Robinson et al., 1982). Iwasaki (1963) and Coleman (1967) reported the rimming of actinolite by glaucophane and vice versa, or stable coexistence of the two amphiboles, in blueschists. More recently, detailed compositional data on these amphiboles have become available for a wide range of blueschist occurrences, equilibrated under pressures of 5–12 kbar, and temperatures of 200–550°C. All such occurrences appear to show Na-amphibole–Ca-amphibole compositional gaps of varying width (see Robinson et al., 1982, Fig. 20).

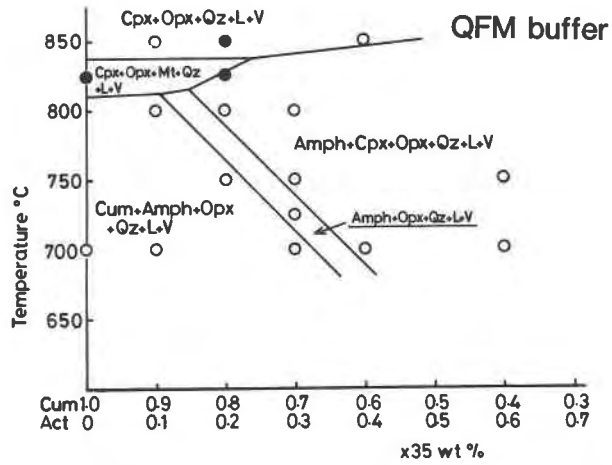

Fig. 6. *T-X* diagram for portion of the join $Cum_{35}(An_{20})_{40}Qz_{25}$-$Act_{35}(An_{20})_{40}Qz_{25}$ (weight proportions) at P_{H_2O} = 5 kbar, f_{H_2} = FMQ. Symbols as for Fig. 2.

Klein (1969) suggested from studies of the composition of amphiboles as a function of metamorphic grade that the Na-amphibole–Ca-amphibole miscibility gap is sensitive to temperature. Brown (1974, 1977), Katagas (1974), and Green and Spiller (1977) all concluded that increase in temperature and/or decrease in pressure associated with the blueschist-greenschist facies transition causes narrowing or closing of the gap. Ernst (1979) suggested that the

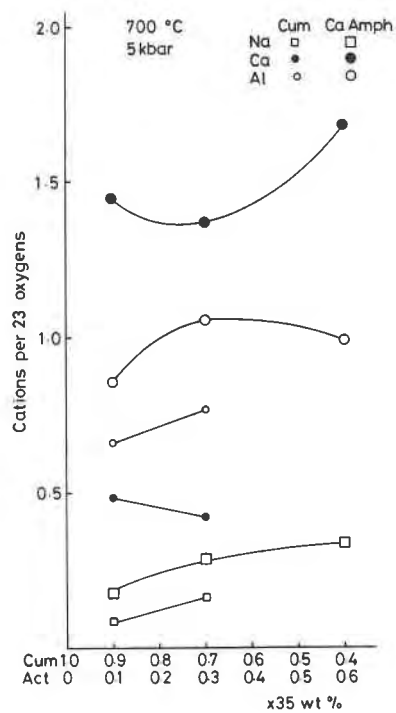

Fig. 7. Variation in proportions of Na, Ca, and Al as a function of system bulk composition for cummingtonites and actinolites-hornblendes in the system Cum-Act-(An_{20})-Qz at 5-kbar P_{H_2O}, 700°C.

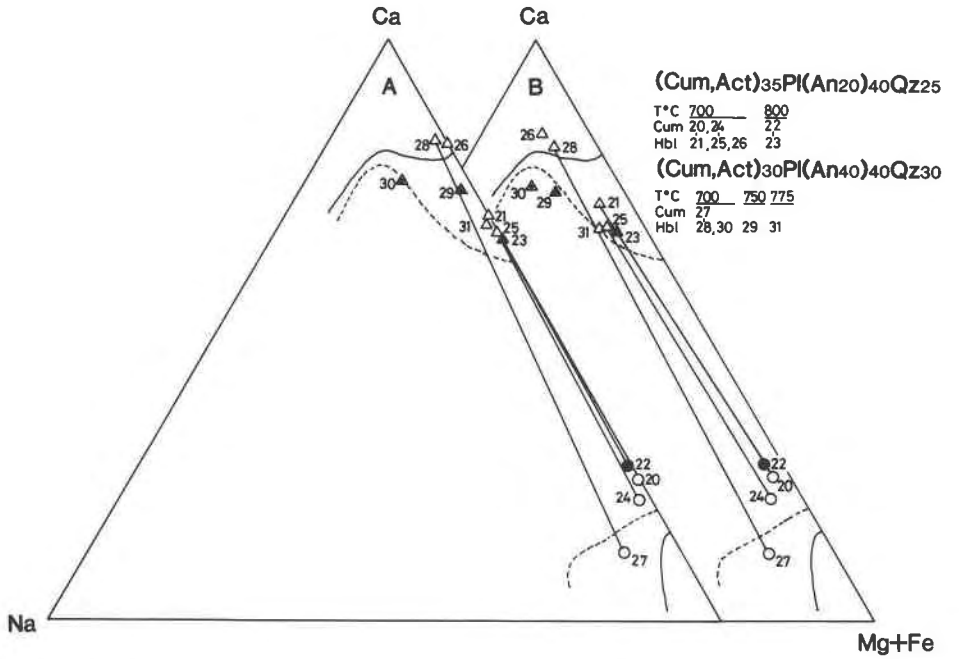

Fig. 8. Relative proportions of Ca, Na, and (Mg + Fe^{2+}) in the M4 site for coexisting amphiboles in the systems $(Cum\text{-}Act)_{35}(An_{20})_{40}Qz_{25}$ and $(Cum\text{-}Act)_{30}(An_{40})_{30}Qz_{30}$. Solid and dashed field boundaries as for Fig. 4. (A) Fe^{2+} equals total Fe. (B) Fe^{2+} and Fe^{3+} (average) calculated by the Spear-Kimball procedures.

gap as observed in blueschists could be closed by the development of Na-Ca (barroisitic) amphibole at around 5–7 kbar, 450°C, but his interpretation of available analytical data was questioned by Robinson et al. (1982).

At temperatures >550°C, Na-amphibole is replaced by Ca-Na amphibole (hornblende) in amphibolite-facies assemblages, and by omphacitic clinopyroxene in eclogites. The apparent lack of Na-amphibole–Ca-amphibole immiscibility under these conditions is consistent with the results of the present study, in which at 5 kbar, 700°C and above, no solvus is observed, even in unusually sodic bulk compositions.

The compositions of coexisting Na-amphiboles and Ca-amphiboles from blueschist assemblages, when plotted in terms of M4-site occupancy (Fig. 4) fall close to the Na-Ca side of the compositional triangle (Robinson et al., 1982, Fig. 20). This is well illustrated for compositions reported by Brown (1974) and Green and Spiller (1977). By contrast, the Na-Ca amphiboles crystallized in the present study plot on a trend from the Ca apex (analysis no. 19) toward the midpoint of the Na–(Mg + Fe^{2+}) side (no. 6), when all Fe is treated as Fe^{2+}. Although this trend moves toward the Na-Ca edge when Fe^{3+} is estimated, the synthetic amphiboles still have considerably higher contents of the cummingtonite molecule than natural equivalents. This presumably reflects their higher temperatures of equilibration. This interpretation is supported by the occurrence of a riebeckite-tremolite from Labrador reported by Klein (1966), which falls near the center of the Ca–Na–(Mg + Fe^{2+}) triangle and on the trend of a solid-solution series of crossite-actinolite type in the present experiments (Fig. 4). Klein considered that this riebeckite-tremolite was produced at considerably higher temperatures than those of blueschist assemblages.

Cummingtonite-actinolite-hornblende relationships

The compositional relationships between Ca-amphiboles (actinolite, hornblende) and Mg-Fe clinoamphiboles (cummingtonites) have been studied by many authors (see Robinson et al., 1982). The two amphiboles coexist in a wide range of metamorphic rocks, especially greenschists and amphibolites (e.g., Klein, 1968; Robinson and Jaffe, 1969; Ross et al., 1969; Stout, 1972; Spear, 1977, 1982) and, much more rarely, in acid igneous rocks (Klein, 1969; Ewart et al., 1971, 1975; d'Arco et al., 1981; Pedersen and Hald, 1982; Wones and Gilbert, 1982). In all these parageneses, representing temperatures within the approximate range 400°C to 750°C and pressures up to 5 kbar, there is a broad miscibility gap between the two amphiboles, with cummingtonite containing a maximum of about 0.4 Ca atoms on a 23-oxygen basis and coexisting Ca-amphibole a minimum of about 1.6 Ca (Robinson et al., 1982). A similar, but generally narrower, miscibility gap is also observed in the experimental assemblages of the present study at 5 kbar, 700–750°C.

The present results are most applicable to the interpretation of the rather diverse cummingtonite-bearing phenocryst assemblages of rhyolites and dacites. Ewart et al. (1971, 1975) subdivided rhyolitic lavas and pumices of the Taupo volcanic zone, New Zealand, into five groups on the basis of ferromagnesian silicate assemblages: (1) Cum + Hbl ± Opx, (2) Hbl + Opx ± Ca-Cpx, (3) Bi +

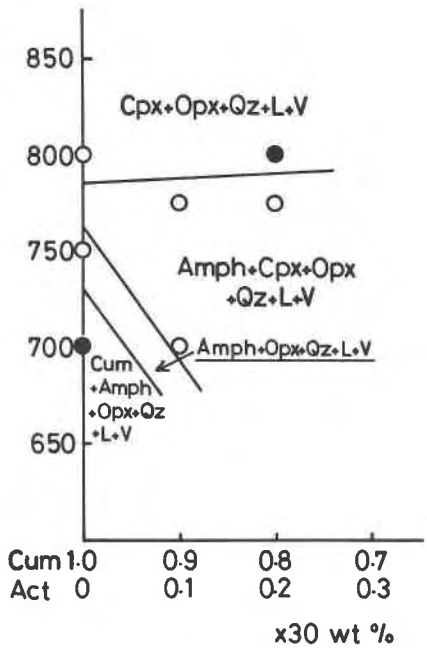

Fig. 9. T-X diagram for portion of the join $Cum_{30}(An_{40})_{40}Qz_{30}$-$Act_{30}(An_{40})_{40}Qz_{30}$ (weight proportions) at P_{H_2O} = 5 kbar, f_{H_2} = FMQ.

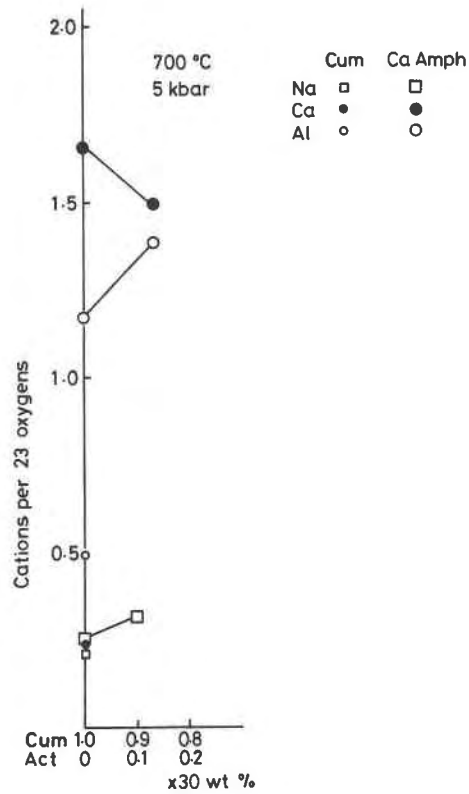

Fig. 10. Variation in proportions of Na, Ca, and Al as a function of system bulk composition for cummingtonites and hornblendes in the system Cum-Act-(An_{40})-Qz at 5-kbar P_{H_2O}, 700°C.

Hbl ± Cum ± Opx, (4) Opx ± Ca-Cpx, and (5) fayalitic Ol ± Opx + Ca-Cpx. D'Arco et al. (1981) described ferromagnesian silicate assemblages similar to (2) and (3) and also Cum + Opx in dacitic pumices from the Lesser Antilles. Pedersen and Hald (1982) recorded an assemblage similar to (3) in an intrusive dacite from the Miocene Kroksfjördur volcano, northwestern Iceland. Using methods developed by Ewart et al. (1971, 1975) and Wood and Carmichael (1973), all these workers have estimated the P_{load}-T-P_{H_2O} equilibration conditions of cummingtonite-bearing phenocryst assemblages as lying within the ranges of 0.7–4.5 kbar and 700–750°C, under conditions of $P_{H_2O} \simeq P_{load}$. All these natural assemblages carry orthopyroxene as the dominant pyroxene accompanying cummingtonite, although Ca-clinopyroxene is sometimes present. The phase relationships applicable in terms of Figure 3, are therefore those with the tie lines Cum-Opx and Ca-Na Amph–Opx stable at the expense of the Cum-Cpx tie line established by the experiments at 2 kbar of Cameron (1975). This suggests maximum pressures of equilibration closer to 5 kbar than 2 kbar.

In Figure 11, the average compositions of cummingtonite-hornblende pairs of the present study are plotted in terms of Ca-Mg-Fe^{2+} ratios and compared with those of natural pairs from igneous and metamorphic rocks. The experimental pairs (Fig. 11A) are plotted both with total Fe as Fe^{2+} (open symbols) and with calculated Fe^{2+} and Fe^{3+} contents (closed symbols). Hornblendes have Mg/Fe_{tot} ratios appreciably higher than those of coexisting cummingtonites, a relationship that is accentuated by the higher estimated Fe^{3+}/Fe^{2+} ratios of the hornblendes (Table 3). The three 700°C pairs appear to define a miscibility gap that narrows toward more magnesian compositions, and this trend is continued by the single 800°C pair (nos. 22, 23).

At 700°C, the amphibole pair defining the narrowest miscibility gap (nos. 20, 21) has nearly 0.5 Ca atoms in M4 sites in cummingtonite and 1.4 Ca in M4 sites in hornblende calculated on a 23-oxygen basis (Table 3). Cummingtonite substitution in the hornblende is approximately 29 mol% (assigning Ca and Na to actinolite and pargasite endmembers). The equivalent figure for the 800°C hornblende is 32%, suggesting that the temperature effect on the miscibility gap is relatively small. Comparison with the estimated maximum of 15% cummingtonite substitution in the actinolites (solid solutions of endmember actinolite and cummingtonite) crystallized at 2-kbar P_{H_2O} by Cameron (1975) suggests that the miscibility gap may narrow with increasing pressure. This suggestion is supported by preliminary experiments in the Cum-Act-Pl-Qz systems at 3-kbar P_{H_2O} (using internally heated high-pressure gas apparatus), which indicate that the stability field of cummingtonite extends to compositions richer in Act component, with lower solubility of cummingtonite in actinolite, than is the case at 5-kbar P_{H_2O}. At 750°C, the stability fields of cummingtonite at 3 and 5 kbar extend

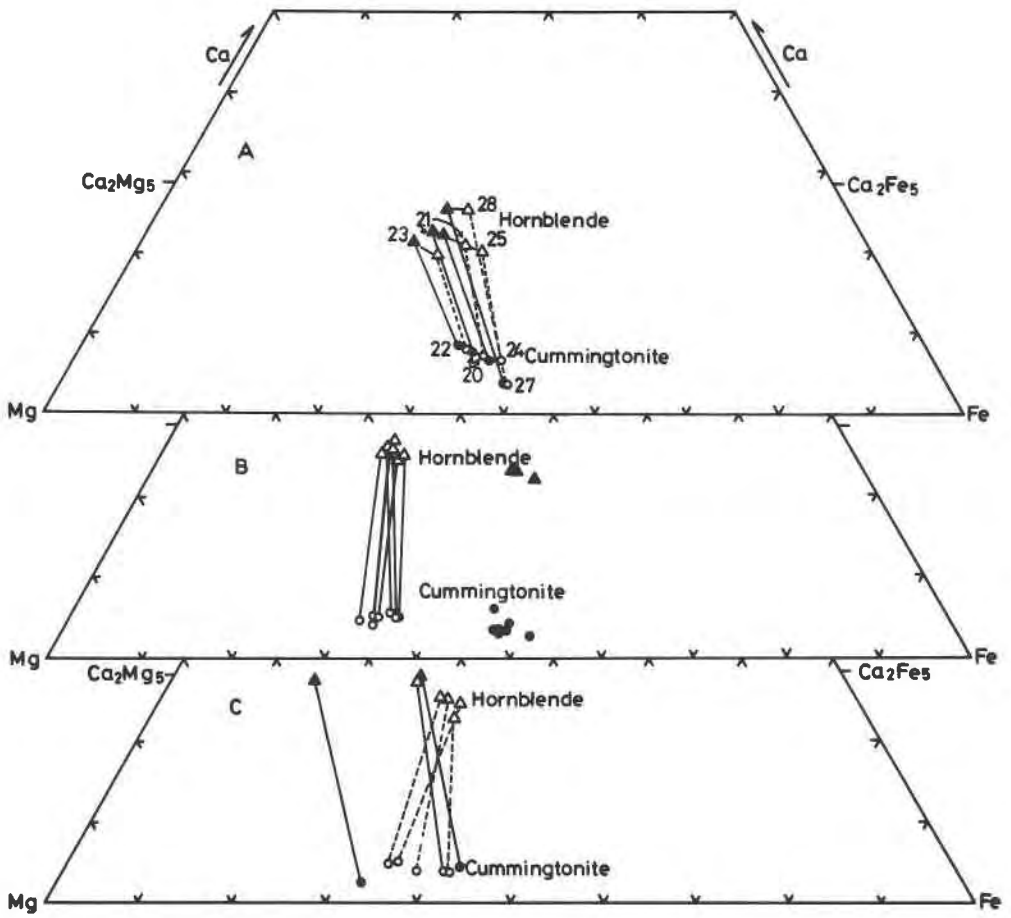

Fig. 11. Amphibole quadrilateral plots of cummingtonite-hornblende pairs from experimental assemblages in the systems Cum-Act-(An_{20},An_{40})-Qz, compared with selected natural pairs. (A) Cummingtonites and actinolitic hornblendes or hornblendes of the experimental assemblages (Table 3), plotted both with Fe^{2+} = total Fe (open symbols) and calculated Fe^{2+} contents (closed symbols). (B) Cummingtonite-hornblende pairs from phenocryst assemblages of rhyolites of the Taupo volcanic zone, New Zealand (open symbols), and a dacite from Martinique, Lesser Antilles (closed symbols)—Ewart et al. (1975), d'Arco et al. (1981). (C) Cummingtonite-hornblende pairs from volcanic rocks from various sources studied by Klein (1968) (open symbols) and an intrusive dacite from the Kroksfjördur volcanic center, northwest Iceland (Pedersen and Hald, 1982) (closed symbols). Four pairs considered by Klein to represent disequilibrium assemblages are distinguished by dashed tie lines.

to maximum bulk CaO contents of 4.3 and 2.7 wt%, respectively.

Pressure dependence of the cummingtonite–Ca-amphibole solvus was previously suggested by Papike et al. (1973) and Cameron (1975). In amphibolites of the Ruby Mountains, Montana, the apparent maximum solubility of cummingtonite in actinolite (~Mg_{60}) is almost 50 mol% (Papike et al., 1973) at temperatures of around 620°C (Ross et al., 1969). Papike and coworkers suggested that mutual solubility of coexisting amphiboles increased with increasing P_{H_2O}, and Cameron (1975) explained this effect by noting that in the system Cum–Act (Mg_{50}), increasing P_{H_2O} would raise the high-temperature boundary of the cummingtonite + actinolite field as observed at 2-kbar P_{H_2O} at the expense of cummingtonite + pyroxene assemblages. This would expose more of the crest of the amphibole solvus and allow enhanced mutual solubility.

The natural cummingtonite-hornblende pairs of Figures 11B and 11C show appreciable differences in orientation of tie lines and apparent width of miscibility gaps, both with respect to one another and to the experimental pairs of Figure 11A. All but the four pairs of Klein (1968) represented by open symbols and dashed tie lines are believed by the original authors to be equilibrium assemblages. In Figure 11B, phenocryst pairs from rhyolites of the Taupo volcanic zone, New Zealand (Ewart et al., 1971, 1975—compositions as recalculated by Powell, 1975) are relatively magnesian (~Mg_{65}—open symbols), with hornblendes slightly more magnesian than cummingtonites and a miscibility gap considerably wider than that of the experimental pairs. Pairs from a Lesser Antilles dacite (d'Arco et al., 1981) have compositions near Mg_{50}, with hornblendes slightly more Fe-rich than cummingtonites, and a miscibility gap similar in width to the experimental

equivalent. Since geothermometry suggests that both the Taupo zone and Lesser Antilles pairs equilibrated at temperatures (700–780°C) similar to those of the experimental pairs, variations in width of the miscibility gap may have pressure significance, with the Taupo zone pairs representing pressures appreciably less than 5 kbar (calculated values of Ewart et al., 1975, are in the range 0.7–3.1 kbar) and Lesser Antilles pairs pressures closer to 5 kbar (the range calculated by d'Arco et al., 1971, is 2.3–4.5 kbar). In Figure 11C, the pairs of Klein (1968) and Pedersen and Hald (1982) defined miscibility gaps much wider than those of the experimental pairs, implying lower pressures and/or lower temperatures of equilibration.

Further evidence for pressures of equilibration of these assemblages will be presented in a companion paper dealing with experimental crystal-liquid phase and compositional relations (Oba and Nicholls, in prep.).

Acknowledgments

We thank A. Hohmann for assistance with microprobe analysis, R. Douglass for preparation of polished sections, and L. Jones, W. Manley, and R. Clarke for manufacture of high-pressure furnace assemblies. W. Conrad reviewed the manuscript. This study was supported by the Australian Research Grants Scheme (Grants E78/15237 and E84/15990) whose assistance is gratefully acknowledged.

References

Brown, E.H. (1974) Comparison of the mineralogy and phase relations of blueschists from the north Cascades, Washington, and greenschists from Otago, New Zealand. Geological Society of America Bulletin, 85, 333–344.

——— (1977) The crossite content of Ca-amphibole as a guide to pressure of metamorphism. Journal of Petrology, 18, 53–72.

Cameron, K.L. (1975) An experimental study of actinolite-cummingtonite phase relations with notes on the synthesis of Fe-rich anthophyllite. American Mineralogist, 60, 375–390.

Coleman, R.G. (1967) Glaucophane schists from California and New Caledonia. Tectonophysics, 4, 479–498.

d'Arco, Ph., Maury, R.C., and Westercamp, D. (1981) Geothermometry and geobarometry of a cummingtonite-bearing dacite from Martinique, Lesser Antilles. Contributions to Mineralogy and Petrology, 77, 177–184.

Ernst, W.G. (1979) Coexisting sodic and calcic amphiboles from high-pressure metamorphic belts, and the stability of barroisitic amphibole. Mineralogical Magazine, 43, 269–278.

Ewart, A. (1971) Notes on the chemistry of ferromagnesian phenocrysts from selected volcanic rocks, central volcanic region. New Zealand Journal of Geology and Geophysics, 14, 323–340.

Ewart, A., Green, D.C., Carmichael, I.S.E., and Brown, F.H. (1971) Voluminous low temperature rhyolitic magmas in New Zealand. Contributions to Mineralogy and Petrology, 33, 128–144.

Ewart, A., Hildreth, W., and Carmichael, I.S.E. (1975) Quaternary acid magma in New Zealand. Contributions to Mineralogy and Petrology, 51, 1–28.

Green, T.H., and Spiller, A.R. (1977) Blue amphibole from Precambrian metabasalts, Savage River, Tasmania. American Mineralogist, 62, 164–166.

Iwasaki, M. (1963) Metamorphic rocks of the Kotu-Bizan area, eastern Sikoku. University of Tokyo Faculty of Science Journal, section II, 15, 1–90.

Katagas, C. (1974) Alkali amphiboles intermediate in composition between actinolite and riebeckite. Contributions to Mineralogy and Petrology, 46, 257–264.

Klein, C. (1966) Mineralogy and petrology of the metamorphosed Wabush iron formation, southwestern Labrador. Journal of Petrology, 7, 246–305.

——— (1968) Coexisting amphiboles. Journal of Petrology, 9, 281–330.

——— (1969) Two-amphibole assemblages in the system actinolite-hornblende-glaucophane. American Mineralogist, 54, 212–237.

Leake, B.E. (1978) Nomenclature of amphiboles. American Mineralogist, 63, 1023–1052.

Papike, J.J., Cameron, K.L., and Shaw, K.W. (1973) Chemistry of coexisting actinolite-cummingtonite and hornblende-cummingtonite from metamorphosed iron formation. Geological Society of America Abstracts with Programs, 5, 763–764.

Pedersen, A.K., and Hald, N. (1982) A cummingtonite-porphyritic dacite with amphibole-rich xenoliths from the Tertiary central volcano at Kroksfjördur, N.W. Iceland. Lithos, 15, 137–159.

Powell, R. (1975) Thermodynamics of coexisting cummingtonite-hornblende pairs. Contributions to Mineralogy and Petrology, 51, 29–37.

Robinson, P., and Jaffe, H.W. (1969) Chemographic exploration of amphibole assemblages from central Massachusetts and southwestern New Hampshire. Mineralogical Society of America Special Paper 2, 251–274.

Robinson, P., Spear, F.S., Schumacher, J.C., Laird, J., Klein, C., Evans, B.W., and Doolan, B.L. (1982) Phase relations of metamorphic amphiboles: Natural occurrence and theory. Mineralogical Society of America Reviews in Mineralogy, 9B, 1–211.

Ross, M., Papike, J.J., and Shaw, K.W. (1969) Exsolution textures in amphiboles as indicators of subsolidus thermal histories. Mineralogical Society of America Special Paper 2, 275–299.

Spear, F.S. (1977) Phase equilibria of amphibolites from the Post Pond Volcanics, Vermont. Carnegie Institution of Washington Year Book 76, 613–619.

——— (1981) An experimental study of hornblende and compositional variability in amphibolite. American Journal of Science, 281, 699–734.

——— (1982) Phase equilibria of amphibolites from the Post Pond Volcanics, Mt. Cube Quadrangle, Vermont. Journal of Petrology, 23, 383–426.

Spear, F.S., and Kimball, K.L. (1984) RECAMP—A FORTRAN IV program for estimating Fe^{3+} contents in amphiboles. Computers in Geosciences, 10, 317–325.

Stout, J.H. (1972) Phase petrology and mineral chemistry of coexisting amphiboles from Telemark, Norway. Journal of Petrology 13, 99–145.

Wones, D.R., and Gilbert, M.C. (1982) Amphiboles in the igneous environment. Mineralogical Society of America Reviews in Mineralogy, 9B, 355–390.

Wood, B.J., and Carmichael, I.S.E. (1973) P_{total}, P_{H_2O} and the occurrence of cummingtonite in volcanic rocks. Contributions to Mineralogy and Petrology, 45, 149–158.

MANUSCRIPT RECEIVED SEPTEMBER 4, 1985
MANUSCRIPT ACCEPTED JULY 8, 1986